An Experimental/Numerical Study of Internal Wave Transmission Across an Evanescent Level

B. R. Sutherland and P. F. Linden

Department of Applied Mathematics and Theoretical Physics, University of Cambridge.

Abstract

Numerical and experimental studies show that a wavepacket of internal gravity waves may be partially reflected from and transmitted into a region where the wave intrinsic frequency is comparable to the background buoyancy frequency. The departure of the propagation behaviour from that predicted by ray theory is examined in detail. In particular, weakly nonlinear effects are shown to play a significant role when horizontally periodic waves are of moderately large amplitude, though such effects are inhibited for waves that are horizontally as well as vertically compact. Some qualitative results of these analyses are presented here.

1 Introduction

Ray theory is often employed to predict the path followed by a packet of internal gravity waves (IGW) in a background with variable flow and stratification. The theory itself employs the WKBJ approximation and consequently is valid only if the vertical wavelength of the waves is much smaller than the length scale of the background variations (for example, see Lighthill [1]). Nonetheless, if a wavepacket propagates into weakly stratified fluid or if the background flow speed changes with height so that the intrinsic frequency of the waves approaches the value of the background buoyancy frequency, then the vertical wavelength increases to infinity and the assumptions of ray theory are violated. Such circumstances occur frequently in nature. For example, by way of numerical simulations, Laprise [2] has demonstrated that considerations of non-WKBJ effects may be crucial to appropriately model the propagation and reflection of mountain waves, and Sutherland [3] has proposed that a potential momentum source for the deep zonal countercurrents in the equatorial oceans may be internal waves generated near the surface that are partially transmitted below the thermocline by a mechanism enhanced by non-WKBJ effects.

In an idealised study of IGW in stationary but non-uniformly stratified fluid in which the profile of the buoyancy frequency, $N(z)$, decreases from N_0 to a value N_+ comparable with the initial wavepacket frequency, ω_0, it was shown that a horizontally periodic wavepacket partially reflected from and transmitted

into the weakly stratified region[4]. Reflection coefficients predicted from linear theory allowing for transient effects agreed well with those determined for a simulated small amplitude wavepacket. For waves of large amplitude, however, IGW reflection was shown to be enhanced for non-evanescent waves (*i.e.* $\omega_0 < N_+$) and it was shown that enhanced IGW transmission of evanescent waves could likewise occur. This nonlinear effect was shown to occur due to the change in phase speed of the waves at their reflecting levels: the phase speed changes as the mean flow is rapidly accelerated then decelerated by the incident waves that first increase then decrease in amplitude as the wavepacket reflects. In their study of non-WKBJ effects upon transient IGW incident upon a critical level, Fritts and Dunkerton [5] referred to this weakly nonlinear wave-mean flow interaction as the "self-acceleration" of the waves. In their study, dissipative processes near the critical level result in permanent changes to the mean flow, in part, due to transient effects. Here, however, dissipative processes are negligible and transient accelerations therefore induce no permanent changes to the mean flow [6, 7, 8], but serve only to modify the characteristics of the waves themselves.

The numerical study of IGW propagation in non-uniform stratification is extended here to include the effects of background shear. In section 2 we describe the numerical model used and report some of the more salient results. Experiments have been performed to examine IGW generated by a vertically oscillating cylinder in salt stratified water. The path followed by these horizontally and vertically compact wavepackets is compared in section 3 with the predictions of ray theory. It is shown that when the buoyancy frequency varies rapidly with height compared with the vertical wavelength of the waves the waves propagate more vertically than predicted. If the buoyancy frequency far from the cylinder reduces to values comparable with the IGW frequency, partial reflection and transmission occurs. The implications of this work are discussed in section 4.

2 Numerical Simulations

Numerical simulations of the fully nonlinear evolution of an IGW wavepacket in a horizontally periodic channel with free-slip upper and lower boundaries are performed by solving the primitive equations for Boussinesq flow restricted to two dimensions, using a code based upon that developed by Smyth and Peltier [9].

In studies with variable background flow, the stratification is assumed constant with $N^2 = 1$ everywhere and the background flow $U(z) = T(z)$ is assumed to have a hyperbolic tangent form such that the flow decreases with height from zero to $-\Delta U$ over a distance characterised by the length scale H:

$$T(z) = -\frac{\Delta U}{2}\left[1 + \tanh\left(\frac{z}{H}\right)\right]. \tag{2.1}$$

In studies with variable stratification the background flow is assumed to be stationary and the stratification is characterised by

$$N^2(z) = 1/[1 - |\vec{k}|T(z)]^2. \tag{2.2}$$

N^2 is defined in this way so that the profile of the ratio, $\Omega(z)/N(z)$, of the wave intrinsic frequency ($\Omega = \omega_0 - k_x U$) to the buoyancy frequency is the same if ΔU is the same for simulations either with shear or with non-uniform stratification. In particular, whether for large z the value of this ratio, $\Omega_+/N_+ = \omega_0 + k_x \Delta U$, is greater than or less than one determines whether or not, respectively, the incident waves from below are evanescent in the upper region.

A vertically compact wavepacket centred about $z_0 = -30$ is superimposed initially on the basic state prescribed by a streamfunction of the form

$$\psi(x,z) = A \exp\left(-|z - z_0|/D\right)) \cos\left(\vec{k} \cdot \vec{x}\right) \tag{2.3}$$

in which the vertical extent of the wavepacket $D = 5$ is chosen to be sufficiently large that the wavepacket supports many vertical waves, but it is sufficiently small that the IGW amplitude is negligible near $z = 0$. The wavenumber vector $\vec{k} = (1, -0.7071)$ corresponds approximately to that of a wavepacket with the largest positive vertical group velocity where $N^2 = 1$. From the dispersion relationship of IGW, the frequency and, with $k_x = 1$, the horizontal phase speed of the wavepacket are approximately $\sqrt{2/3}$.

The effect of nonlinearity is illustrated in Figure 1 which shows profiles of the perturbation kinetic energy (PKE) and the perturbation density field at the end of two simulations of IGW in uniformly stratified shear flow: in diagrams a) and b) for small amplitude waves ($A = 0.02$) and in diagrams c) and d) for large amplitude waves ($A = 0.3$). In both simulations the background flow well above $z = 0$ is set so that the incident wavepacket is evanescent in the region, specifically, where $\Omega_+/N_+ \simeq 1.02$.

In corresponding simulations of IGW in stationary, but variable N^2 fluid the same qualitative behaviour is observed if $\Omega_+/N_+ \simeq 1.02$, though in this case the transmitted waves propagate with smaller vertical group velocity and a larger proportion of the wavepacket is reflected. A measure of the proportion that is reflected is determined at the end of the simulation by comparing the perturbation kinetic energy of the wavepacket associated with a downward momentum flux to the perturbation kinetic energy of the the entire wave field. Figure 2 shows the reflection coefficients as a function of Ω_+/N_+ for small (dashed lines) and large (solid lines) amplitude waves in simulations with a) uniform stratification and shear, and b) non-uniform stratification and stationary flow.

As mentioned earlier, the transmission and reflection of waves is nonlinearly enhanced due to the effect of the wave-induced mean flow upon the phase speed of the waves. If the waves are horizontally compact, however, the effect is significantly retarded. Simulations have been performed for vertically and horizontally compact wavepackets whose envelopes in the horizontal are Gaussian with standard deviation σ:

$$\psi(x,z) = A \exp\left(-|z - z_0|/D)\right) \exp\left(-x^2/2\sigma^2\right) \cos\left(\vec{k} \cdot \vec{x}\right) \tag{2.4}$$

Figure 2c) shows the reflection coefficient for small and large amplitude waves in stationary but variable N^2 fluid for such a wavepacket with $\sigma = 2\lambda_x$, twice the

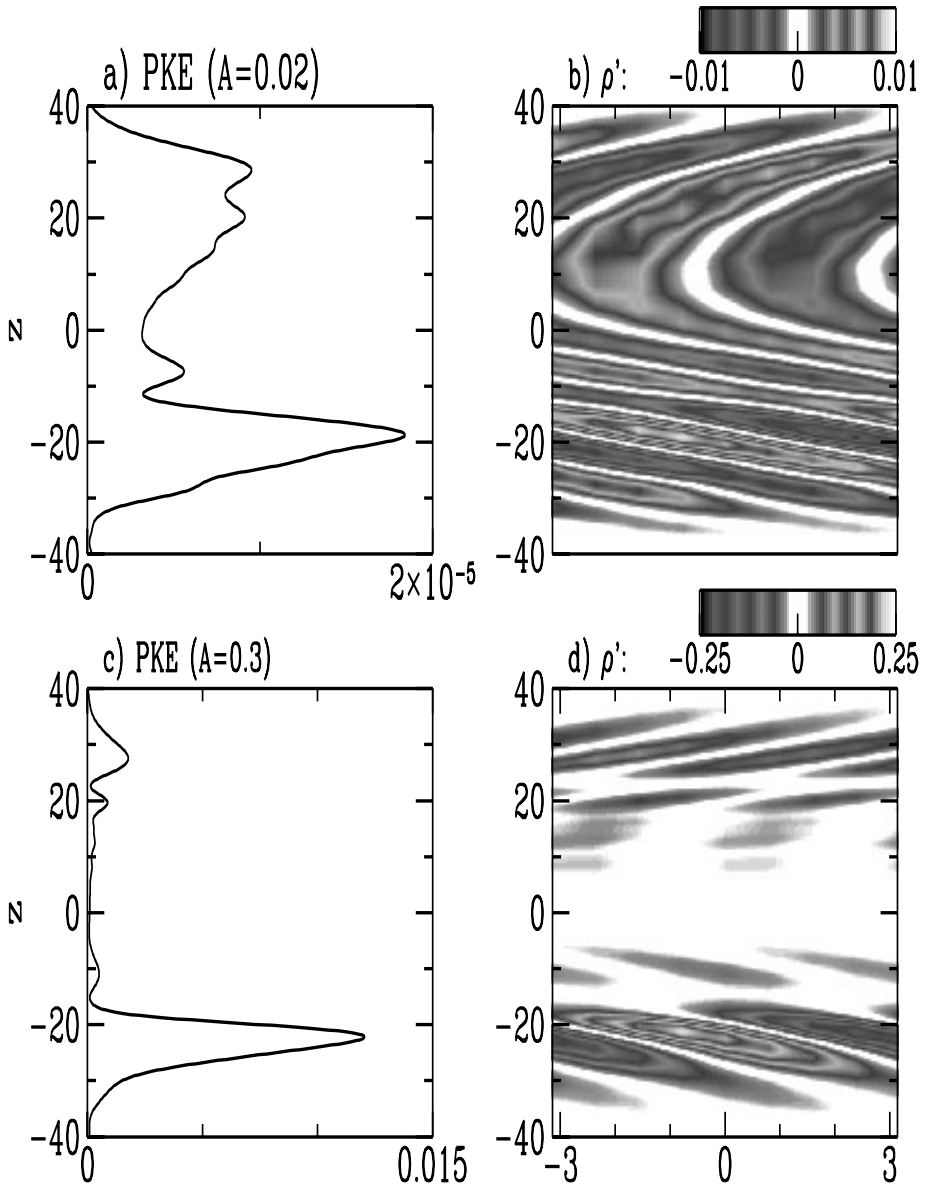

Figure 1. In a) and c) perturbation kinetic energy profiles, and b) and d) perturbation density fields are shown at time $t = 150$ in simulations with $\Omega_+/N_+ \simeq 1.02$. The waves in a) and b) are of small amplitude ($A = 0.02$), and in c) and d) they are of large amplitude ($A = 0.3$). Note that contours of the perturbation density are shown on a scale 25 times smaller for small amplitude waves than for large amplitude waves.

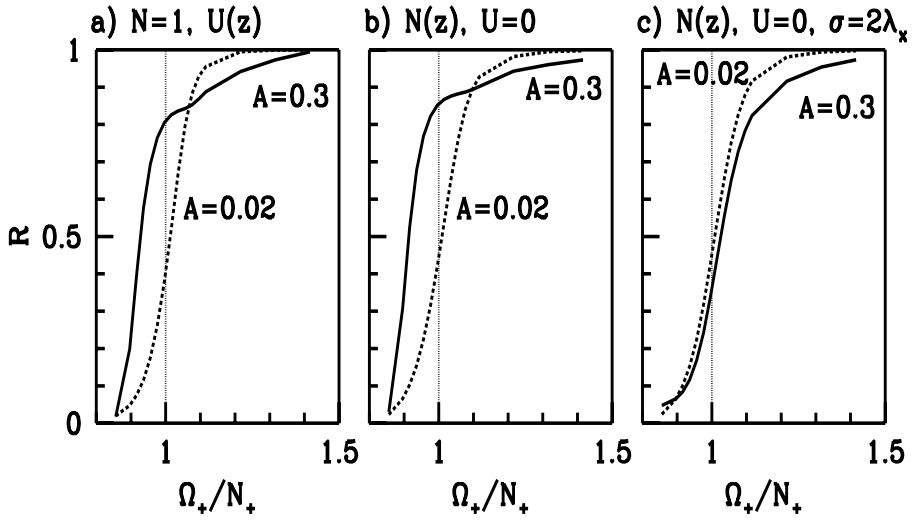

Figure 2. Reflection coefficients determined at time $t = 150$ for large (solid lines) and small (dashed lines) amplitude waves in simulations of horizontally periodic, vertically compact IGW with a) uniform stratification and shear, and b) non-uniform stratification and stationary flow. In c) the coefficients are calculated similarly for a simulation of horizontally and vertically compact IGW in non-uniformly stratified stationary flow. The vertical dotted line in each diagram indicates the critical value of the ratio of the wave intrinsic frequency to the background buoyancy frequency for $z \gg 0$, Ω_+/N_+. When this ratio is greater than 1, the incident wavepacket is evanescent.

horizontal wavelength of the initial waves. The graph shows that the proportion of reflected waves is similar for both large and small amplitude waves when the incident waves are not evanescent in the region well above $z = 0$ (*i.e.* $\Omega_+/N_+ < 1$). Nonetheless, wave transmission is nonlinearly enhanced when the incident waves are evanescent (*i.e.* $\Omega_+/N_+ > 1$). Future work will quantify these results further.

3 Laboratory Experiments

Non-WKBJ effects are examined in laboratory experiments for IGW generated by a vertically oscillating cylinder in salt stratified water. Waves so generated have frequently been studied [10, 11, 12, 13, 14]. In particular, an oscillating cylinder in uniformly stratified fluid is well known to produce a wave pattern in the shape of a Saint Andrew's Cross [1, 15]. Our experiments are performed in a racetrack shaped tank with test section 240 cm long, 40 cm deep, and 20 cm wide [16]. Uniform stratification is set up using a "double-bucket" system, and variable stratification is established by changing the salinity of one bucket during the filling process. Typically the tank is filled to a depth of 35 cm. The density

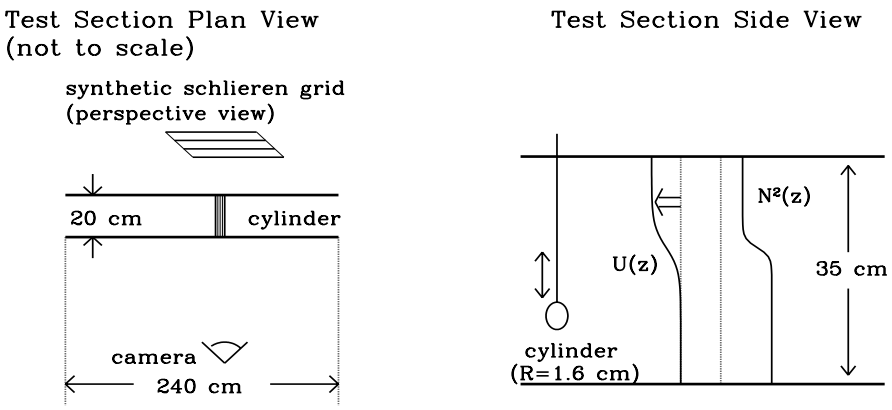

Figure 3. Schematic of the experimental set-up.

profile is measured between 9 and 31 cm from the bottom of the tank using a mechanically traversed conductivity probe which, in one pass samples the local conductivity every 0.2 millimetre at a rate of 100 samples per second. A PVC cylinder of radius 1.6 cm generates IGW by oscillating vertically with its axis horizontal and spanning the width of the test section, the axis in its equilibrium position being situated 11.4 cm above the bottom of the tank. The cylinder oscillates with a peak to peak amplitude of up to 0.7 cm for a range of periods between 1 and 50 seconds. We examine the upward propagating waves emanating to the right of the cylinder. An angled barrier spanning the width of the test section with one end resting on the bottom of the tank is inserted with its other end near the cylinder to block bottom reflections from the right and downward propagating waves. For some experiments (not reported here) a shear flow is established near the surface by an Odell-Kovasznay drive [17]: two sets of intermeshed horizontal disks situated between 30 and 35 cm height rotate in opposite directions, thus driving fluid by viscosity with a minimum of vertical mixing.

Visualisation of the waves is accomplished using a "synthetic schlieren" system. The visualisation is relatively simple and inexpensive to set up: a back-illuminated grid of horizontal black lines is positioned well behind the test section of the tank and a CCD camera is positioned on the opposite side of the tank focussed on the grid lines through the salt stratified water, as shown schematically in Figure 3. Because the index of refraction of salt water varies with salinity the stretching and compressing of isopycnals due to the passage of IGW deflects light rays passing through the tank between the grid and the camera. Stretched isopycnals deflect light upward; compressed isopycnals deflect light downward. By comparing the initial position of the grid lines with their position when waves are present, waves with amplitudes as small as tenths of millimeters can be visualised. The comparison is done by instantaneously digitising and processing the images from a CCD camera using "DigImage", a image processing system

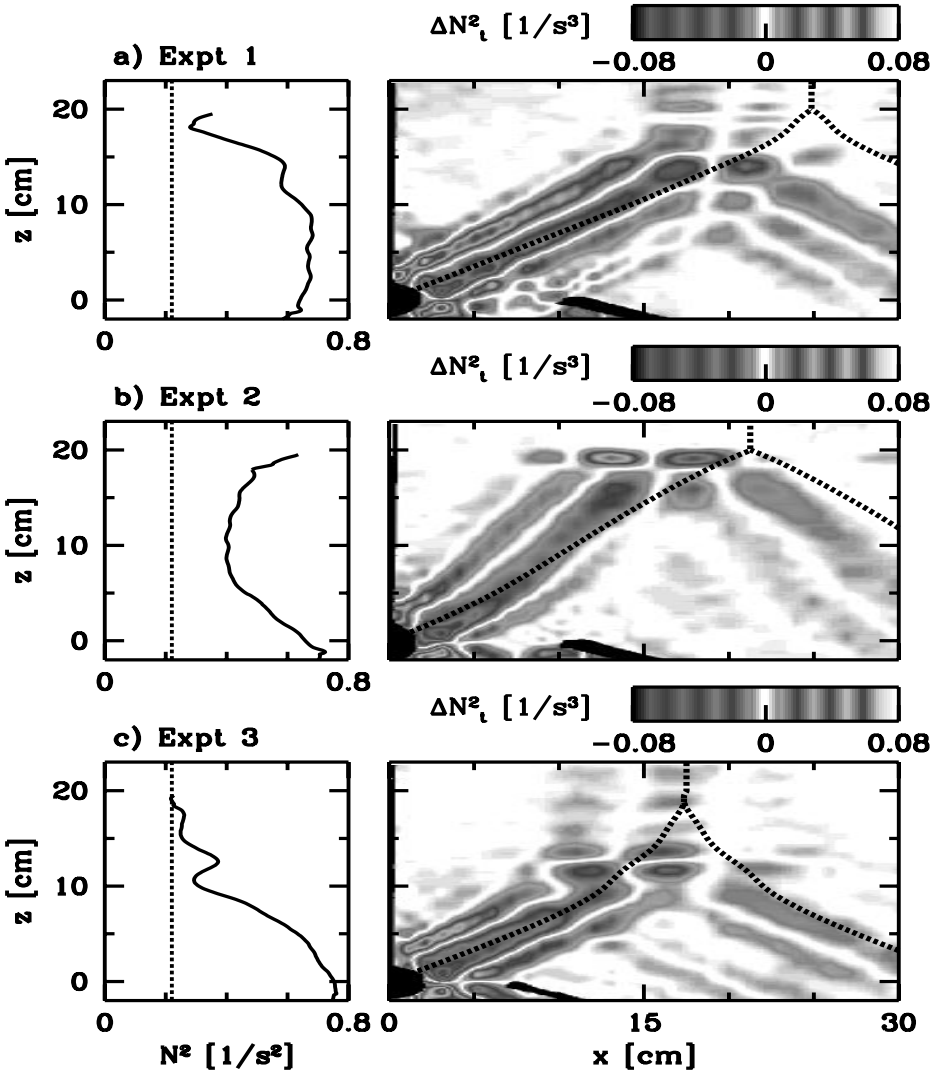

Figure 4. Three laboratory experiments of IGW propagation in non-uniformly stratified fluid. In each case the cylinder oscillates at the origin with frequency 0.47 rad/s and amplitude 0.7 cm. In a) the background stratification varies slowly with height near the source, in b) it reduces rapidly with height, and in c) the buoyancy frequency far from the source is comparable to the wave frequency. Each diagram shows the background N^2 profile with the vertical dashed line representing the squared frequency of the IGW. To the right of each profile are fields of the time rate of change of N^2 shown 100 s after the cylinder begins oscillating. The bold dashed lines superimposed on each field is the path followed by an IGW wavepacket as predicted by ray theory.

developed by Dr. Stuart Dalziel[18]. A powerful feature of this technique is that it provides a method by which to measure non-intrusively and quantitatively the amplitude of the two-dimensional wave field everywhere in space and time to the resolution of the camera and video.

With this set-up, we have studied the propagation of IGW into weakly stratified fluid. As expected, IGW have larger vertical tilt as they propagate into more weakly stratified fluid and reflect from a mixed region near the surface. Figure 4 shows the results of three experiments of IGW propagating into weakly stratified, stationary fluid. In each experiment, the cylinder oscillates at a frequency 0.47 rad/s and with peak to peak amplitude 0.7 cm. The background N^2 profiles are shown for each experiment with $z = 0$ corresponding to the position of the cylinder axis at equilibrium. To the right of these are shown the fields of the time rate of change of N^2 after the cylinder has oscillated continuously for 100 s. A comparison of the path of the waves with that predicted by ray theory (the dashed line superimposed on each field) shows that the waves tend to propagate more vertically than predicted, particularly when N^2 varies rapidly with height compared with the vertical wavelength of the waves. In particular, Figure 4b demonstrates the limitations of the WKBJ approximation.

In experiments for which the buoyancy frequency reduces with height to a value comparable to the wave frequency, IGW are observed to undergo partial transmission and reflection. For example, Figure 4c shows weak partial IGW reflection well below the evanescent level. This reflection occurs continuously and does not result from transient effects in the usual sense.

The numerical model described in section 2 has been adapted to simulate the experimental set-up by adding a local external forcing term to the vertical velocity equation. The forcing is uniform over a circular patch centred at the origin with the same radius as the cylinder in the experiment, and the forcing magnitude varies sinusoidally in time with the same frequency. The simulated waves follow the same path as those generated experimentally, partially reflecting from and transmitting into weakly stratified fluid. After calibrating for the amplitude of the simulated waves, the average vertical flux of horizontal momentum is determined for waves near the cylinder (τ_0), at $z = 3.6$ cm averaged between $x = 0$ and 16 cm, for transmitted waves (τ_+) at $z = 31.6$ cm, and for reflected waves (τ_-) at $z = 3.6$ cm averaged between $x = 16$ and 35 cm.

Figure 5 shows that an approximately constant positive momentum flux is associated with waves near the cylinder shortly after it begins to oscillate. The fluctuations about the mean flux occur on the same frequency as the oscillation frequency. As the waves propagate into the weakly stratified fluid a positive momentum flux is associated with the transmitted waves and a negative momentum flux is associated with the reflected waves. The magnitude of the mean reflected wave momentum flux is approximately double in magnitude that of the transmitted waves and exhibits larger fluctuations about the mean.

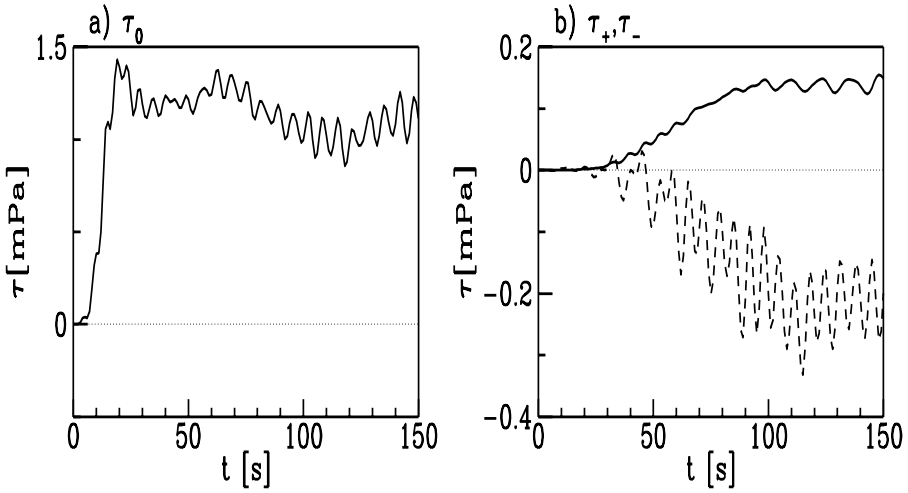

Figure 5. From a numerical simulation of the laboratory experiment shown in Figure 4c, vertical fluxes of horizontal momentum ($\tau = \rho_0 \langle u'w' \rangle_x$) are determined over time for a) incident, and b) transmitted (solid line) and reflected (dashed line) IGW.

4 Discussion and Conclusions

We have shown numerically and experimentally that the behaviour of IGW deviates significantly from that predicted by ray theory when the assumptions of the WKBJ approximation are violated due to either rapid background variations or weakly nonlinear effects. Of course, there is no reason to expect ray theory to apply to IGW under such circumstances. Nonetheless, general circulation models of the atmosphere presently adopt its predictions in order to parametrise subgrid-scale gravity wave drag, even under circumstances in which the theory fails (for example, see McFarlane [19], Palmer *et al* [20]). This work introduces a programme of study that will attempt to lead to improved parametrisation schemes. In order to model simply the effect of partial reflection and transmission, reflection coefficients have been calculated for wavepackets of different geometries (vertically compact and either horizontally periodic or horizontally compact) and amplitudes. In either shear flow with uniform stratification or stationary flow with non-uniform stratification, the coefficients differ by only a small amount if the profiles of $\Omega(z)/N(z)$ are the same in both cases. If $\Omega_+/N_+ \simeq 1$, however, the reflection coefficient for large amplitude IGW is almost double that for small amplitude IGW if they are horizontally periodic. This nonlinearly enhanced reflection is inhibited for horizontally compact wavepackets of width comparable to the horizontal wavelength.

The numerical work leading to these conclusions requires that the wavepacket to be vertically compact and that the transient self-acceleration of the waves

plays a crucial role. However, in laboratory experiments of IGW generated by an oscillating cylinder and incident upon a weakly stratified region, partial reflection and transmission occurs with steady periodic IGW. This may result from transience when the horizontal wavelength is comparable with the wavepacket width. The same study shows that IGW tend to tilt more vertically than predicted by ray theory when the stratification varies rapidly with height, compared with the vertical wavelength. In future work the numerical model will be adapted to include non-Boussinesq effects appropriate to the middle atmosphere.

The authors would like to thank Stuart Dalziel and Graham Hughes who developed and helped adapt the synthetic schlieren system used extensively here. This work has been supported by the Natural Environment Research Council (NERC) grant GR3/09399.

Bibliography

[1] Lighthill, M. J. (1978). *Waves in Fluids.* Cambridge University Press, Cambridge, England, 504 pp.

[2] Laprise, J. P. R. (1993). An assessment of the WKBJ approximation to the vertical structure of linear mountain waves: implications for gravity wave drag parameterization. *J. Atmos. Sci.*, **50**, 1469–1487.

[3] Sutherland, B. R. (1996). The dynamic excitation of internal gravity waves in the equatorial oceans. *J. Phys. Oceanogr.*, **26**, 3214–3235.

[4] Sutherland, B. R. (1996). Internal gravity wave radiation into weakly stratified fluid. *Phys. Fluids*, **8**, 430–441.

[5] Fritts, D. C. and Dunkerton, T. J. (1984). A quasi-linear study of gravity-wave saturation and self-acceleration. *J. Atmos. Sci.*, **41**, 3272–3289.

[6] Eliassen, A. and Palm, E. (1960). On the transfer of energy in stationary mountain waves. *Geofys. Publ.*, **22**, 1–23.

[7] Andrews, D. G. and McIntyre, M. E. (1976). Planetary waves in horizontal and vertical shear: The generalized Eliassen-Palm relation and the mean flow acceleration. *J. Atmos. Sci.*, **33**, 2031–2048.

[8] Andrews, D. G. and McIntyre, M. E. (1978). An exact theory of nonlinear waves on a Lagrangian-mean flow. *J. Fluid Mech.*, **89**, 609–646.

[9] Smyth, W. D. and Peltier, W. R. (1989). The transition between Kelvin-Helmholtz and Holmboe instability: An investigation of the overreflection hypothesis. *J. Atmos. Sci.*, **46**, 3698–3720.

[10] Görtler, H. (1943). Über eine schwingungserscheinung in flüssigkeiten mit stabiler dichteschichtung. *Z. angew. Math. Mech.*, **23**, 65–71.

[11] Mowbray, D. E. and Rarity, B. S. H. (1967). A theoretical and experimental investigation of the phase configuration of internal waves of small amplitude in a density stratified liquid. *J. Fluid Mech.*, **28**, 1–16.

[12] Stevenson, T. N. and Thomas, N. H. (1969). Two-dimensional internal waves generated by a travelling oscillating cylinder. *J. Fluid Mech.*, **36**, 505–511.

[13] Koop, C. G. (1981). A preliminary investigation of the interaction of internal gravity waves with a steady shearing motion. *J. Fluid Mech.*, **113**, 347–386.

[14] Nicolaou, D. , Liu, R. , and Stevenson, T. N. (1993). The evolution of thermocline waves from an oscillatory disturbance. *J. Fluid Mech.*, **254**, 401–416.

[15] Voisin, B. (1991). Internal wave generation in uniformly stratified fluids. Part 1. Green's function and point sources. *J. Fluid Mech.*, **231**, 439–480.

[16] Redondo, J. M. R. . Internal and external mixing in a stratified-shear flow. In Fernholz, H. H. and Fiedler, H. E. , editors, *Advances in Turbulence 2* 198. Springer-Verlag, (1989).

[17] Odell, G. M. and Kovasznay, L. S. G. (1971). A new type of water channel with density stratification. *J. Fluid Mech.*, **50**, 535–543.

[18] Dalziel, S. B. (1993). Rayleigh-Taylor instability: experiments with image analysis. *Dyn. Atmos. Oceans*, **20**, 127–153.

[19] McFarlane, N. A. (1987). The effect of orographically excited gravity wave drag on the general circulation of the lower stratosphere and troposphere. *J. Atmos. Sci.*, **44**, 1775–1800.

[20] Palmer, T. N. , Shutts, G. J. , and Swinbank, R. (1986). Alleviation of a systematic westerly bias in general circulation and numerical weather prediction models through an orographic gravity drag parametrization. *Quart. J. Roy. Meteor. Soc.*, **112**, 1001–1039.